ELSEVIER

Journal of Alloys and Compounds 224 (1995) 194–198

Journal of ALLOYS AND COMPOUNDS

Preparation of perovskite-type oxides by thermal decomposition of heteronuclear complexes, $\{Ln[Fe(CN)_6]\cdot nH_2O\}_x$, (Ln = La ~ Ho)

Yoshihiko Sadaoka [a,*], Kazuaki Watanabe [a], Yoshiro Sakai [a], Masatomi Sakamoto [b]

[a] *Department of Applied Chemistry, Faculty of Engineering, Ehime University, Matsuyama 790, Japan*

[b] *Department of Chemistry, Faculty of Science, Yamagata University, Yamagata 990, Japan*

Received 21 November 1994; in final form 23 December 1994

Abstract

Perovskite-type oxides with submicron particle size were prepared by thermal decomposition of heteronuclear cyano complexes. Dehydration and decomposition of CN-bridged structure were performed by heating at ~300 °C in air, generating vitreous phases containing carbonates. For the complexes comprising La, Pr, Nd and Sm, submicron-sized particles of perovskite-type oxide directly formed from a vitreous phase. Single phase of perovskite-type oxide was formed by heating at ~600 °C of the complex with La. For the complexes comprising Gd, Dy and Ho, heat-treatment at ~300 °C led to formation of a vitreous phase containing carbonate and no perovskite-type oxide. By increasing the calcining temperature, a mixture of single oxides (Fe_2O_3 and Ln_2O_3) and perovskite-type oxides was formed at lower temperatures and single-phase perovskite-type oxide at higher temperatures. The formation temperature of the perovskite-type oxide increased with decreasing lanthanoid ion radius.

Keywords: Perovskite-type oxides; Thermal decomposition; Heteronuclear complexes

1. Introduction

Fine powders of perovskite oxides are interesting materials, which exhibit characteristics (high nonstoichiometry and mixed conductivity, i.e. both ionic and electronic charge carriers) relevant to practical applications. Various preparation techniques have been developed [1–6], including the sol-gel technique. Recently, we proposed a new method based on thermal decomposition of heteronuclear complexes and found that homogeneous perovskitic oxides with high specific surface areas were formed at low temperatures [7–9]. Bailey et al. [10] reported that the three-dimensional networks of $\{Ln[Fe(CN)_6]\cdot 5H_2O\}_x$ are constructed by Fe(III)-CN-La(III) linkages. The hexagonal structure of $[LaFe(CN)_6]\cdot 5H_2O$ was confirmed by Bailey et al., by Hulliger et al. [11] and also by Kietaibl and Petter [12]. The structural configuration of Fe and Ln ions is very similar to the corresponding perovskitic oxide. Thus the formation of perovskitic oxides by calcination of the corresponding complexes is expected to progress easily by diffusion of Fe and Ln ions.

In the present work, we examine the thermal decomposition behavior of $\{Ln[Fe(CN)_6]\cdot 5H_2O\}_x$ and the crystal growth of perovskitic $LnFeO_3$.

2. Experimental

The complex $La[Fe(CN)_6]\cdot 5H_2O$ (a reddish-orange powder) was synthesized by mixing aqueous solutions of equal molar amounts of lanthanum(III) nitrate hydrate and potassium hexacyanoferrate(III) with continuous stirring [13]. The resulting reddish-orange precipitate was washed with water, ethanol and diethyl ether and dried in air. The potassium content of the purified complex was less than 0.05 wt.% by atomic absorption analysis. The other complexes were synthesized in the same way. For the heavy lanthanoid metals such as Er or Yb, the chemical composition of the complexes was not well reproducible. Elemental analysis was applied to determine the contents of carbon, hydrogen and nitrogen. The metal contents were determined by EDTA titration of a dilute nitric acidic solution of the oxide. The thermal decomposition behaviour was examined by thermogravimetrical analysis

* Corresponding author.

SSDI 0925-8388(95)01531-0

(TG), infrared spectroscopy (IR) and X-ray diffraction (XRD). The heat-treated samples were prepared by holding at various temperatures in ambient air after raising the temperature at 5 °C min^{-1}. Crystal structure and particle shape were examined by XRD and SEM, respectively. Specific surface areas were determined by the BET method using nitrogen as an adsorbate.

3. Results and discussion

3.1. Thermal decomposition behaviour of complexes

The TG curve for the complexes with a heating rate of 5 °C min^{-1} in ambient air was examined (Fig. 1). For $\{La(Fe(CN)_6]\cdot 5H_2O\}_x$, dehydration begins at approximately 50 °C, and a quasi-plateau region was observed in the temperature range of 250–300 °C. The weight loss at 280 °C is about 20 wt.%, which is in good agreement with the value (20.43 wt.%) calculated by assuming the formation of anhydrate. Further heating caused a weight loss due to exothermal decomposition of the cyanide groups, as also confirmed by DTA, followed by a short plateau. Exothermal decomposition begins at 345 °C. Further heating up to 620 °C induced a further gradual decrease in weight. In this region some short plateaus were detected. At temperatures above 620 °C the weight remained constant. The temperature corresponding to the final weight is defined as Tf_{TG}. The total weight loss (44.29 wt.%) in the last plateau range agreed very well with that (44.95 wt.%) calculated for perovskite-type $LaFeO_3$ or a 1:1 mixture of Fe_2O_3 and La_2O_3.

The estimated lattice constants of the samples decomposed at around Tf_{TG} are summarized in Table 1, and agree reasonably with the values reported by Geller and Wood [14] and Eibschutz [15]. When *Pnma* is applied, the *b*-lattice and *c*-lattice parameters decrease

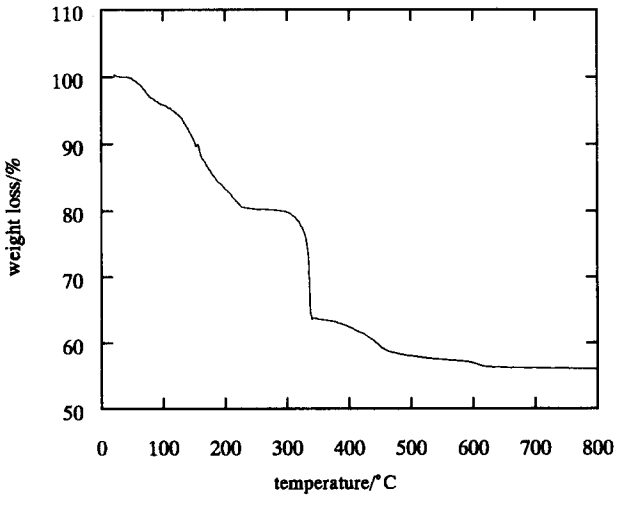

Fig. 1. TG result of $La[Fe(CN)_6]\cdot 5H_2O$.

Table 1
Structural parameters of prepared $LnFeO_3$

Starting material	Calcination temperature (°C)	a (nm)	b (nm)	c (nm)
$La[Fe(CN)_6]\cdot 5H_2O$	620	0.5557	0.7848	0.5561
$Pr[Fe(CN)_6]\cdot 4H_2O$	670	0.5576	0.7786	0.5480
$Nd[Fe(CN)_6]\cdot 4H_2O$	700	0.5577	0.7752	0.5445
$Sm[Fe(CN)_6]\cdot 4H_2O$	750	0.5587	0.7708	0.5392
$Eu[Fe(CN)_6]\cdot 4H_2O$	780	0.5598	0.7682	0.5367
$Gd[Fe(CN)_6]\cdot 5H_2O$	800	0.5601	0.7664	0.5344
$Tb[Fe(CN)_6]\cdot 5H_2O$	820	0.5595	0.7639	0.5325
$Ho[Fe(CN)_6]\cdot 5H_2O$	830	0.5584	0.7604	0.5270

Sys.; orthorhombic.

monotonically with decreasing radius of Ln ions, while the *a*-lattice parameter has a tendency to increase. Furthermore, the changes in the XRD patterns of some complexes were examined. The XRD patterns were obtained at room temperature. In Fig. 2(a) and (b) the results for $[LnFe(CN)_6]\cdot nH_2O$ (Ln = La and Dy) decomposed at several temperatures for 30 min are shown. The lattice constant of perovskite-type oxide is uninfluenced by the calcining/decomposing temperature (< 1000 °C). For $[LaFe(CN)_6]\cdot 5H_2O$ heated at 400 °C, some peaks attributed to perovskite-type $LaFeO_3$ were observed. When the complex was treated at higher temperatures the intensity of peaks attributed to $LaFeO_3$ was enhanced, a broad band at $2\Theta \sim 30.0°$ was not detected, and all observed signals were assigned to perovskite-type $LaFeO_3$. Similar results were obtained for the complexes with Ln = Pr, Nd and Sm. For $[LnFe(CN)_6]\cdot nH_2O$ (Ln = Gd, Dy and Ho) only a broad band at $2\Theta \sim 31.0°$ was observed when the samples were heated at about 700 °C. For the samples heated at about 750 °C some weak peaks attributed to perovskite-type $LnFeO_3$, Ln_2O_3 and Fe_2O_3 were detected. A heat treatment at higher temperatures induced an enhancement in intensity of peaks of perovskite-type $LnFeO_3$ and the disappearance of peaks of Ln_2O_3 and Fe_2O_3. For the sample calcined for 30 min the correlation between the intensity of peaks of perovskite-type oxide and the calcination temperature was examined. The formation temperature (Tf_{XRD}) of perovskite-type oxide was estimated by extrapolation. These results are summarized in Fig. 3 together with Tf_{TG}. Furthermore, carbonates were not detected by XRD. Thus the carbonates detected at the perovskite-type $LnFeO_3$ by IR are formed mainly on the surface due to exposure to ambient air.

3.2. Microstructure

The microstructures of the perovskite type oxides prepared by decomposition of the complexes at various temperatures for 24 h are shown in Fig. 4. For example,

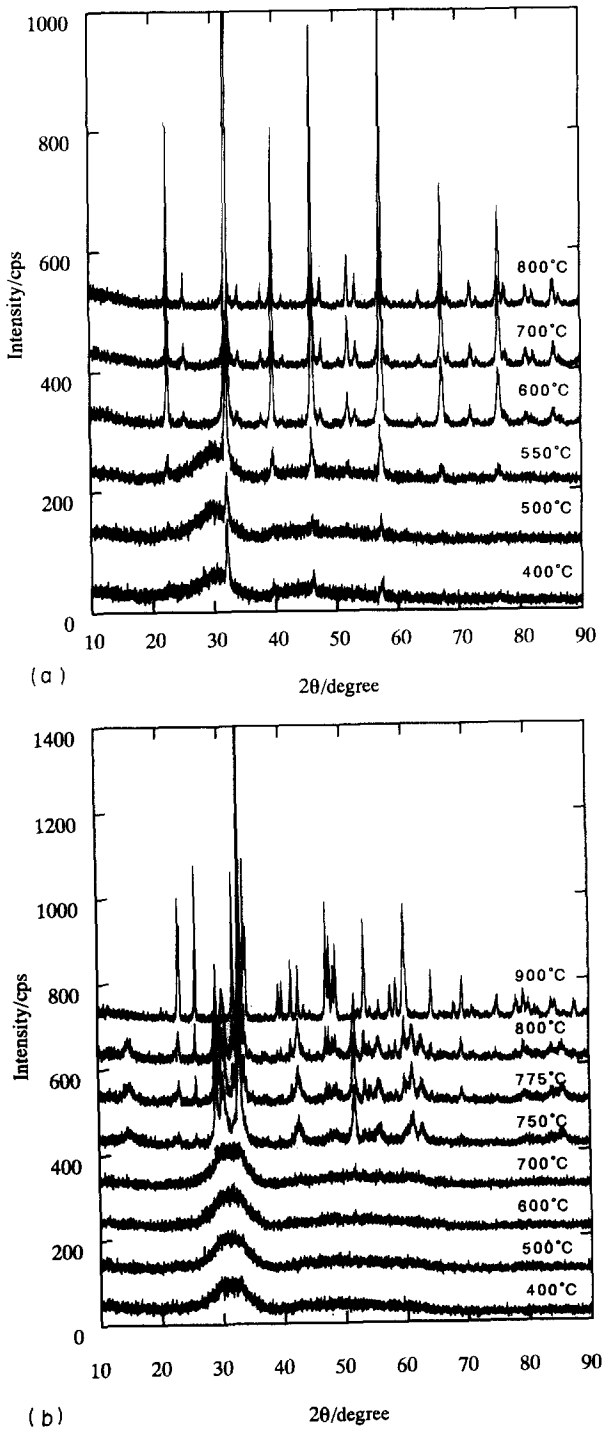

Fig. 2. XRD patterns of: (a) calcined $La[Fe(CN)_6]\cdot 5H_2O$; (b) calcined $Dy[Fe(CN)_6]\cdot 5H_2O$. Calcining temperature is shown in the figure.

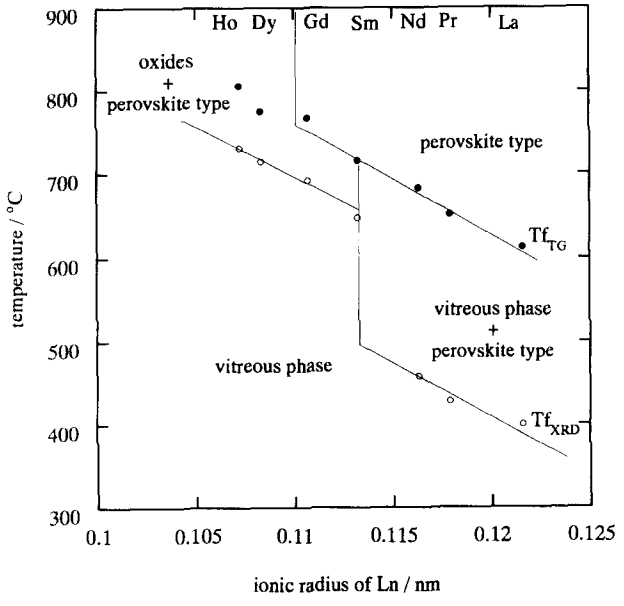

Fig. 3. Correlation between ionic radius of Ln^{3+} and Tf_{TG}, Tf_{XRD}.

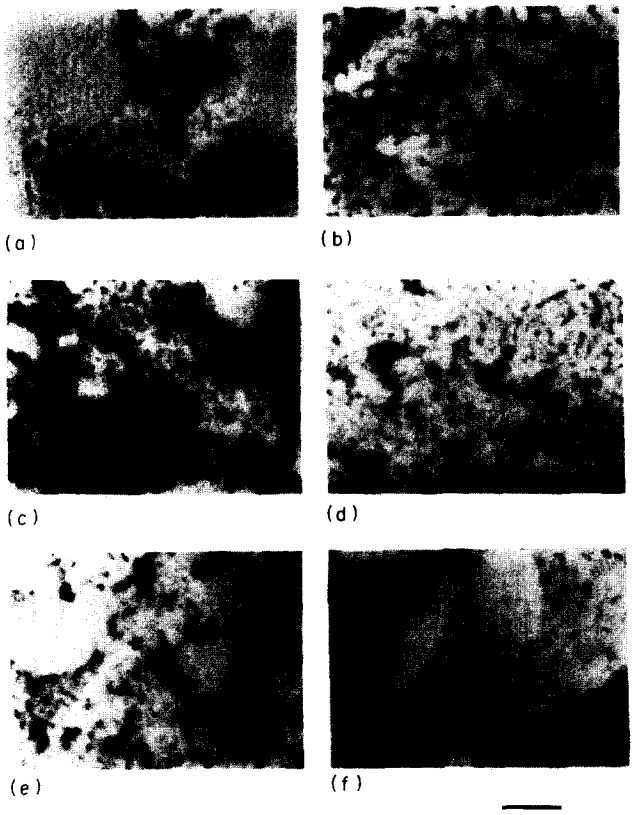

Fig. 4. SEM images of $LnFeO_3$ (bar = 1 μm). Calcining temperatures: (a) $LaFeO_3$, 620 °C for 24 h; (b) $LaFeO_3$, 900 °C for 2 h; (c) $PrFeO_3$, 670 °C for 24 h; (d) $NdFeO_3$, 700 °C for 24 h; (e) $GdFeO_3$, 800 °C for 24 h; (f) $HoFeO_3$, 830 °C for 24 h.

the mean particle diameter of the $LaFeO_3$ obtained by decomposition of the complex at 1000 °C for 10 min is approximately 200 nm as found by SEM. It is well known that metallic oxides may be prepared by thermal decomposition of carbonates or hydroxides, and that their physicochemical properties are determined by the temperature at which they are formed and by the duration of the calcination. For example, the crystal growth of magnesium oxide from $Mg(OH)_2$ proceeds proportionally to $t^{1/n}\exp(-E/kT)$ (t = calcination time, E = activation energy for the crystal growth) [16]. In Fig. 5, the relation between $\log(d/\mu m)$ and $1/T$ is plotted for $LaFeO_3$ prepared by decomposition for 10 min; the

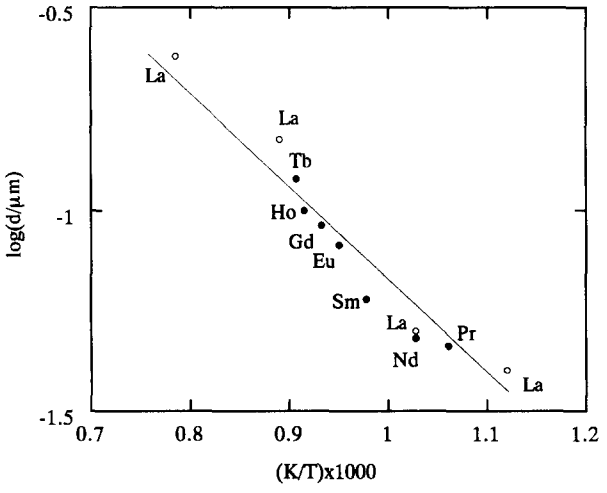

Fig. 5. Correlation between mean particle diameter and calcining temperature.

value of the activation energy is 20 kJ mol^{-1}. It seems that the mean diameter is uninfluenced by the ionic radius of Ln^{3+} and only dependent on the calcination temperature for constant calcination times. As has been demonstrated, the mean diameter is also dependent on the time; the mean diameter of $LaFeO_3$ particles is 200 nm for 10 min and 320 nm for 2 h calcination at 1000 °C.

3.3. IR spectroscopic characterization

In order to characterize the decomposition product of the $\{Ln[Fe(CN)_6]\cdot nH_2O\}_x$ complexes, IR spectra were recorded in transmittance mode for the samples dispersed in KBr discs and in reflectance mode for the compressed powders. The results are shown in Fig. 6(a) and (b). For the complex $\{La[Fe(CN)_6]\cdot nH_2O\}_x$, a ν(CN) stretching band at about 2100 cm^{-1} and a $\delta(H_2O)$ band at about 1620 cm^{-1} were observed. For the sample heated at 400 °C in air, the ν(CN) stretching band could not be observed. Instead, bands attributable to carbonate groups were observed in the 1300–1500 cm^{-1} region. In the transmittance mode the bands attributable to carbonate groups disappeared by heating at 600 °C or higher and ν(MO) stretching bands at about 550 cm^{-1} appeared. In the reflectance mode, on the other hand, the ν(CN) stretching band disappeared after heating at 400 °C or higher, the bands attributable to carbonate groups remained constant and a new broad adsorption band in the 3700–3000 cm^{-1} region, attributed to adsorbed water, was detected even for the sample heated at 800 °C. For the complexes with lanthanoid ions with smaller ionic radii, similar spectral changes in the transmittance mode after heat treatment were found, and the disappearance temperature of absorption bands attributed to carbonate increased with a decrease in the radius of lanthanoid ion. In the reflectance mode, the existence of carbonates

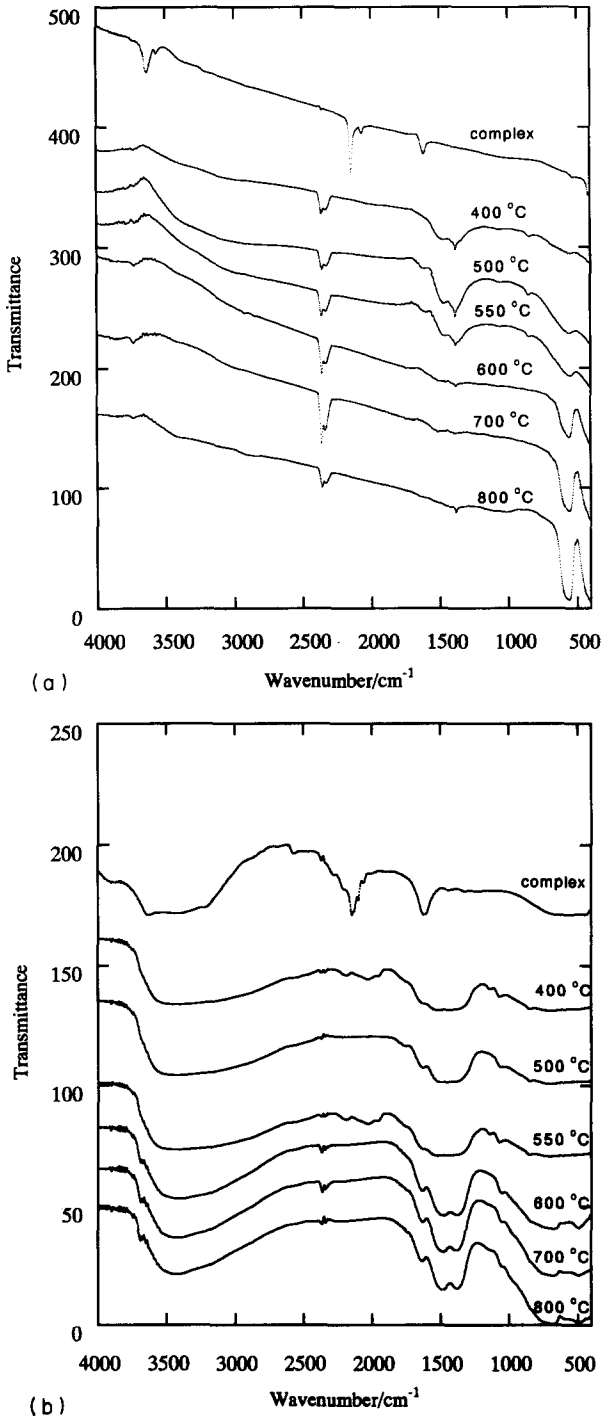

Fig. 6. IR spectra observed in air of $La[Fe(CN)_6]\cdot 5H_2O$ calcined at various temperatures: (a) transmittance mode; (b) reflectance mode.

was confirmed for all examined samples (Ln = La ~ Ho) heated at 800 °C or higher.

In both transmittance and reflectance modes, the absorption bands in the 1300–1500 cm^{-1} region were clearly observed for the samples calcined at Tf_{TG} or below. Thus dehydration and decomposition of the CN-bridged structure proceed by heating at about 300 °C in air, generating a vitreous phase containing carbonates. The carbonates gradually decompose with an increase

in the calcining temperature up to Tf_{TG}. For the samples calcined at a higher temperature ($> Tf_{TG}$), the intensity of the absorption band in the transmittance mode attributed to carbonates is considerably lower than that in the reflectance mode. Furthermore, the intensity of the bands in the reflectance mode is higher than that for the sample calcined at below Tf_{TG}, and splitting of the bands becomes more clear.

For the samples calcined at Tf_{TG} or higher, most of the carbonate decomposes. At the same time single-phase perovskite-type oxide forms for Ln = La, Pr, Nd, and Sm, and a mixture of Fe_2O_3, Ln_2O_3 and perovskite-type oxide for Ln = Gd, Tb, Dy and Ho. The carbonate is formed by exposure to ambient air at room temperature. For comparison, perovskite-type $LaFeO_3$ was prepared by sintering of a 1:1 mixture of La_2O_3 and Fe_2O_3 at various temperatures above 800 °C. For samples sintered at 1000 °C or lower a mixture of perovskite-type oxide, La_2O_3 and Fe_2O_3 was obtained. The content of La_2O_3 and Fe_2O_3 decreased with an increase in temperature, and by sintering at 1100 °C or higher, a single phase of perovskite-type oxide was obtained. The mean particle diameter was 0.6 and 1.6 μm for the 1:1 mixture of La_2O_3 and Fe_2O_3 sintered at 1000 and 1200 °C respectively. These samples showed sharp absorption bands in the 3000–4000 cm^{-1} region, which correspond to surface –OH species, while any broad band could not be detected in ambient air. In addition, some sharp absorption bands were also detected in the 1650–1000 cm^{-1} and 750–450 cm^{-1} region.

Thus calcination at higher temperatures induces dehydration, which involves the condensation of adjacent surface hydroxyl groups. The dehydroxylation of the surface results in formation of a layer of superficial oxygen species, which may be expected to be more reactive than the lattice oxygen towards gases such as CO_2 in ambient. The surface of the particles obtained from the decomposition of the heteronuclear complex is more active to chemisorption of CO_2, leading to the formation of carbonate ions, than that of the particles obtained from sintering of the 1:1 oxide mixture. A more detailed characterization is now in progress by X-ray photoelectron spectroscopy.

Acknowledgements

The present work was supported by a Grant-in-Aid for Scientific Research on Priority Areas "New Development of Rare Earth Complex" No. 06241257 and 06241106 from The Ministry of Education, Science and Culture.

References

[1] H. Oyabashi, T. Kuudo and T. Gejo, *Jpn. J. Appl. Phys., 13* (1974) 1.
[2] T. Nakamura, M. Misono, T. Uchijima and Y. Yoneda, *Nippon Kagaku Kaishi,* (1980) 1679.
[3] M. Yoshimura, S.T. Song and S. Somiya, *Yogyo Kyokaishi, 90* (1982) 91.
[4] H.-M. Zhang, Y. Teraoka and N. Yamazoe, *Chem. Lett.* (1987) 665.
[5] S. Nakayama, H. Kuroshima and Y. Sadaoka, *New Ceramics* (1991) 73.
[6] A. Furusaki, H. Konno and R. Furuichi, *Nippon Kagaku Kaishi* (1992) 612.
[7] M. Sakamoto, Y. Komoto, H. Hojo and T. Ishimori, *Nippon Kagaku Kaishi* (1990) 887.
[8] S. Nakayama and M. Sakamoto, *J. Ceram. Soc. Jpn., 100* (1992) 342.
[9] M. Sakamoto, K. Matsuki, R. Ohsumi, Y. Nakayama, Y. Sadaoka, S. Nakayama, N. Matsumoto and H. Okawa, *J. Ceram. Soc. Jpn., 100* (1992) 1211.
[10] W.E. Bailey, R.J. Williams and W.O. Milligan, *Acta Crystallogr., B29* (1973) 1365.
[11] F. Hulliger, M. Landolt and H. Vetsch, *J. Solid State Chem., 18* (1976) 283.
[12] H. Kietaibl and W. Petter, *Helv. Phys. Acta, 47* (1974) 425.
[13] S. Nakayama, M. Sakamoto, K. Matsuki, Y. Okimura, R. Ohsumi, Y. Nakayama and Y. Sadaoka, *Chem. Lett.* (1992) 2145.
[14] S. Geller and E.A. Wood, *Acta Crystallogr., 9* (1956) 563.
[15] M. Eibschutz, *Acta Crystallogr., A32* (1976) 751.
[16] Y. Kotera, T. Saito and M. Terada, *Bull. Chem. Soc. Jpn., 36* (1963) 195.